

Metal-organic chemical vapor deposition of high-dielectric-constant praseodymium oxide films using a cyclopentadienyl precursor

Hiroki Kondo,^{1,a)} Shinnya Sakurai,¹ Mitsuo Sakashita,¹ Akira Sakai,² Masaki Ogawa,³ and Shigeaki Zaima¹

¹Graduate School of Engineering, Nagoya University, Furo-cho, Chikusa-ku, Nagoya 464-8603, Japan

²Graduate School of Engineering Science, Osaka University, 1-3 Machikaneyama-cho, Toyonaka, Osaka 560-8531, Japan

³EcoTopia Science Institute, Nagoya University, Furo-cho, Chikusa-ku, Nagoya 464-8603, Japan

(Received 12 August 2009; accepted 24 November 2009; published online 6 January 2010)

Praseodymium (Pr) oxide films were grown by metal-organic chemical-vapor-deposition (CVD) using $\text{Pr}(\text{EtCp})_3$. Using H_2O as an oxidant, Pr_2O_3 films with columnar structures are formed and its C concentration can be reduced to about one-tenth compared with the case using O_2 . Activation energy of 0.37 eV is derived for this CVD using H_2O . This CVD-Pr oxide film deposited at 300 °C has a dielectric constant of 26 ± 3 . Furthermore, conduction band offset of 1.0 ± 0.1 eV and trap levels of 0.40 ± 0.02 and 0.22 ± 0.02 eV in the CVD- $\text{Pr}_2\text{O}_3/\text{Si}$ structure were also determined by current conduction characteristics. © 2010 American Institute of Physics. [doi:10.1063/1.3275706]

Further scaling of ultralarge-scale-integrated circuits devices requires gate dielectrics with a subnanometer-order equivalent oxide thickness and, therefore, oxide materials having higher dielectric constant more than Hf oxides are required. Rare-earth metal (Re) oxides, such as a praseodymium (Pr) oxide is one of the promising candidates with a dielectric constant more than 30.¹ Additionally, it has been reported that Pr oxide is substantially an excellent insulator.² However, chemical vapor deposition (CVD) and atomic layer deposition (ALD) techniques for pure Re metal oxide films with a high dielectric constant have not been established yet, although those of silicates and aluminates were reported in several papers.³⁻⁵

β -diketonate precursors [$\text{Re}(\text{DPM})_x$] have been conventionally used for the CVD and ALD. Since their melting points are more than 200 °C, they are usually supplied by sublimation.^{6,7} However, the amounts of those sublimated precursors are usually unstable, and it is too difficult to control them. Furthermore, interfacial reactions with substrates easily occur since $\text{Re}(\text{DPM})_x$ includes oxygen in itself. Therefore, tris[ethyl-cyclopentadienyl]Pr [$\text{Pr}(\text{EtCp})_3$] with a melting point of 72 °C is used in this study. It can be stably delivered by a conventional bubbling system. CVD growth of Pr oxides using $\text{Pr}(\text{EtCp})_3$ was investigated and, H_2O vapors and O_2 gases are compared as an oxidant.

N-type Si(100) wafers were used as a substrate, and subjected with conventional chemical cleaning using RCA solutions. After dilute-HF treatments to remove native oxides, Pr oxide films were deposited by CVD using $\text{Pr}(\text{EtCp})_3$. $\text{Pr}(\text{EtCp})_3$ and H_2O vapors were introduced into the deposition chamber by a bubbling system using a carrier gas of N_2 . The $\text{Pr}(\text{EtCp})_3$ and H_2O were stored in the bottles set to 120 and 40 °C, and the carrier gas flows of N_2 were 10 and 5 SCCM, respectively. O_2 gas was also used as an oxidant for comparison. The O_2 gas flow was 10 SCCM. The CVD growth was carried out at temperatures from 200 to 400 °C. Metal oxide semiconductor (MOS) capacitors with Pt top electrodes ($1.6\text{--}3.0 \times 10^{-4}$ cm²) were fabricated to measure

capacitance-voltage (C - V) and leakage current density-electric field (J - E) characteristics. Any annealing treatment was not subjected to the MOS samples after the CVD and deposition of the Pt gate electrodes.

Figure 1 shows O 1s and C 1s photoelectron spectra of Pr oxide films analyzed by x-ray photoelectron spectroscopy (XPS) after the sputtering by Ar ions for 500 s. In this experiment, 10.1 and 30 nm thick Pr oxide films were formed by the CVD processes for 30 and 10 min using H_2O and O_2 , respectively. The peaks at binding energies of 530.5 and 529.0 eV are attributed to Pr_2O_3 and PrO_2 , respectively.⁸⁻¹⁰ As is well known, Re metal oxides have a high moisture-absorption characteristic. Large peaks related to $\text{Pr}(\text{OH})_3$ were also observed at around 531.5 eV before the surface sputtering. However, intensities of those peaks drastically decreased by the surface sputtering for 500 s, and thereafter shapes of the O 1s peaks are almost similar after the following sputtering. Therefore, the peaks at around 531.5 eV appearing after the sputtering for over 500 s are attributed to PrSiO formed at interfacial regions. Since relative intensity of PrO_2 peak to Pr_2O_3 peak decreases with decreasing take-off-angle of photoelectrons, it is deduced that PrO_2 components mainly exist at the surface regions. In Fig. 2, C 1s intensities are normalized by total intensities of Pr3d peaks. Peaks at around 290 and 285 eV correspond to C–O and C–C

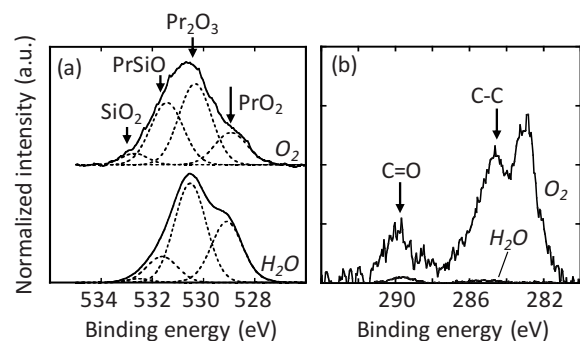


FIG. 1. (Color online) O 1s and C 1s photoelectron spectra of Pr oxide films deposited using (a) O_2 and (b) H_2O . The take-off angle of photoelectrons is 90°.

^{a)}Electronic mail: hkondo@alice.xtal.nagoya-u.ac.jp.

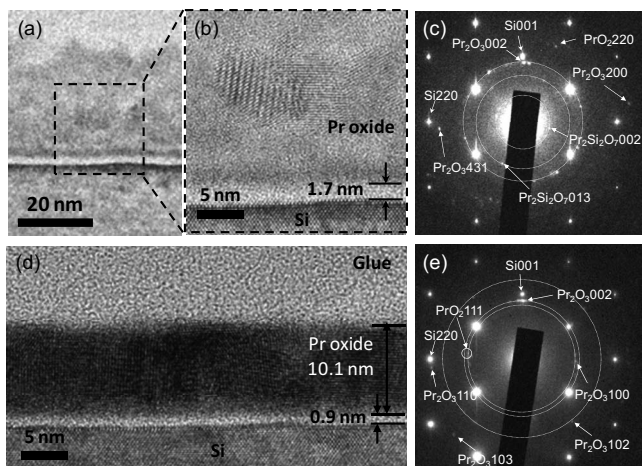


FIG. 2. TEM images and TED patterns of CVD-Pr oxide/Si samples. Pr oxide films were deposited using O_2 [(a)–(c)] and H_2O [(d)–(e)].

bonding states.¹¹ Although peaks at around 283 eV are not clear now, it can be guessed that they come from C–Pr bonding. By using H_2O , not only C–O but also C–C peaks drastically decrease compared to the O_2 case. This means that an incorporation of undecomposed EtCp-ligands is suppressed using H_2O . The decrease in C concentration was also confirmed by Auger electron spectroscopy, in which C concentration of the CVD-Pr oxide film formed using H_2O is 2%, that for the O_2 case is 19%. It is suggested that hydrogen atoms effectively suppress polymerization and deposition of EtCp-ligands onto the sample surfaces.

Figure 2 is transmission electron microscopy (TEM) images and transmission electron diffraction (TED) patterns of the same CVD-Pr oxide/Si samples shown in Fig. 1. In the case of O_2 , the film surface is rough and the film is partially crystallized as observed in Figs. 1(a) and 1(b). On the other hand, it is found that a uniform Pr oxide film with columnar structures is formed by the CVD using H_2O . According to the TED pattern, a hexagonal Pr_2O_3 is oriented onto the Si(001) surface; $Pr_2O_3(002) \parallel Si(001)$. Considering the TEM and XPS results, it is considered that the polycrystalline Pr_2O_3 film is formed using H_2O , although a small amount of PrO_2 exists on the surface region. Thickness of the Pr oxide film formed using H_2O is less than half smaller than that of the O_2 sample despite longer deposition time. It is guessed that crystallization developed in the longer deposition time of the CVD using H_2O . The interlayer thickness of the H_2O sample is 0.9 nm, and it is smaller than that of the O_2 sample.

Figure 3 is growth temperature dependence of Pr-oxide thickness measured by ellipsometry method. Pr-oxide films were deposited by the CVD using H_2O for 1 min. At temperatures of 300 °C and below, activation energy of Pr-oxide growth is obtained to be 0.37 eV. It is guessed that this obtained activation energy is related to a ligand exchange reaction of EtCp in the $Pr(EtCp)_3$ precursor to OH in the H_2O , although details of reaction processes between $Pr(EtCp)_3$ and H_2O are not clear yet. On the other hand, at a temperature of 400 °C, Pr-oxide thickness decreases compared with that at 300 °C. As the reason of this thickness decrease, it is suggested that amount of $Pr(EtCp)_3$ supplied to the substrate surface decreases due to its thermal decomposition in the gas phase.

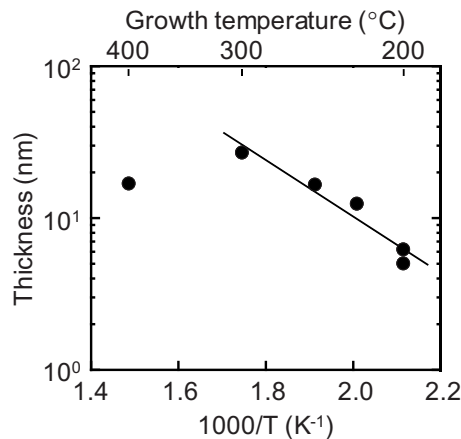


FIG. 3. Growth temperature dependence of Pr-oxide thickness. Pr-oxide films were deposited using H_2O for 1 min.

Figure 4 shows (a) J - E and (b) C - V characteristics in Pt/CVD-Pr oxide/Si MOS capacitors, in which the Pr oxides were formed at 300 °C using H_2O and O_2 , and their TEM images are shown in Fig. 2. The J - E characteristics were measured at the accumulation conditions so that the surface potentials of the substrates were negligibly small. Measurement frequency of the C - V characteristics is 100 kHz. In Fig. 4(a), the leakage current density drastically decreases in the case of CVD using H_2O although its thickness is smaller as shown in Fig. 2. Additionally, hysteresis of C - V characteristics hardly appeared in the case of CVD using H_2O . In the case of the Pr oxide formed using H_2O , capacitance equivalent thickness is 2.4 ± 0.2 nm, and effective dielectric constant including an interlayer is 18 ± 1 . On the other hand, accumulation capacitance does not appear well for the O_2 case due to high leakage currents at the high gate voltage region. According to the XPS results, Pr silicate interlayers exist between the Pr oxide films and Si substrates. Dielectric constant of this Pr silicate interlayer is not clear at this time, however, assuming that it is similar to SiO_2 (3.9), the dielectric constant of Pr oxide film formed using H_2O is obtained to be 26 ± 3 . Although this is just a rough estimation, these calculated values indicate that this Pr oxide formed using $Pr(EtCp)_3$ and H_2O has a dielectric constant of about 20 or more. Figure 5 shows (a) Fowler–Nordheim (F–N) and (b) Poole–Frenkel (P–F) plots of the leakage current through the CVD-Pr oxide formed using H_2O . According to the analysis of this J - E characteristic, a F–N tunneling current is dominant at electric field regions from 1.0 to 2.0 MV/cm. A conduction band offset between the Pr oxide and Si substrate is obtained to be 1.0 eV, which is consistent to the previously

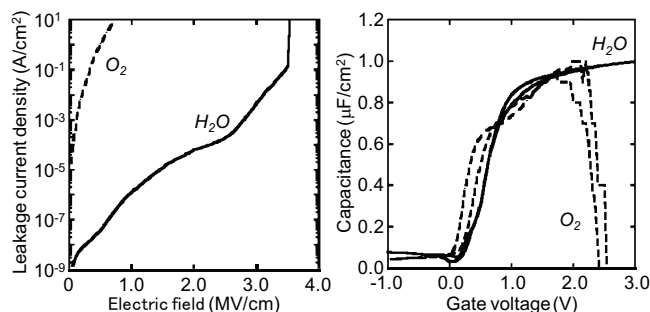


FIG. 4. (a) Leakage J - E and (b) C - V characteristics in Pt/CVD-Pr oxide/Si MOS capacitors. Pr oxide films were deposited using O_2 and H_2O .

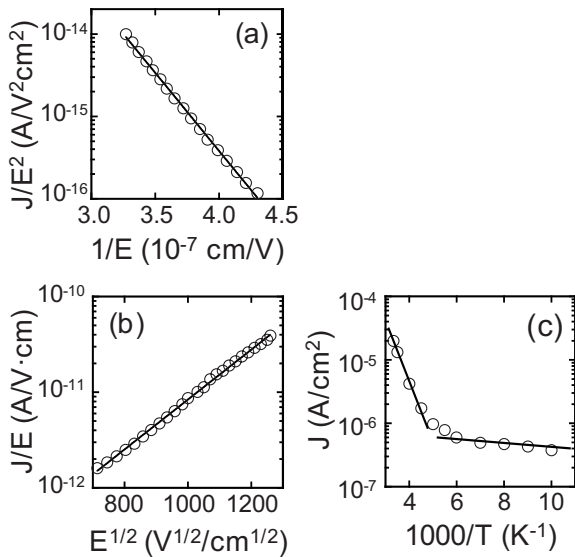


FIG. 5. (Color online) (a) F–N and (b) P–F plots of J - E characteristic at 300 K, and (c) Arrhenius plot of the P–F current at 2 V.

reported for the Pr_2O_3 formed by electron beam evaporation.¹² As shown in Fig. 5(b), a P–F current is dominant above 3.0 MV/cm. A dielectric constant of 23 ± 3 obtained from the slope of the fitted line is almost equal to that from the C - V characteristic. Arrhenius plot of this P–F current is shown in Fig. 5(c). Assuming effective mass of tunneling electrons of 0.5 and dielectric constant of the Pr oxide of 23, energy levels of trapping states are obtained to 0.22 and 0.40 eV below the conduction band edge of the Pr oxide. From these results, it is concluded that, as a result of reduction in C concentration in the CVD using H_2O , the Pr_2O_3

film with low current leakage and high dielectric constants can be obtained.

CVD growth in Pr_2O_3 films using $\text{Pr}(\text{EtCp})_3$ and their electrical properties were reported. The C concentrations of CVD-Pr oxide films were drastically reduced using H_2O as an oxidant, and consequently hexagonal- Pr_2O_3 films with columnar structures are formed. The Pr_2O_3 film with low C concentration, small current leakage, and high dielectric constant can be formed on Si substrates by the CVD using $\text{Pr}(\text{EtCp})_3$ and H_2O .

This work was partly supported by the Ministry of Education, Culture, Sports, Science, and Technology, through a Grant-in-Aid for Scientific Research for Priority Areas, under Grant No. 18063012.

¹H. J. Osten, J. P. Liu, P. Gaworzewski, E. Bugiel, and P. Zaumseil, *Tech. Dig. - Int. Electron Devices Meet.* **2000**, 653.

²J. Dąbrowski, V. Zavodinsky, and A. Fleszar, *Microelectron. Reliab.* **41**, 1093 (2001).

³A. Sakai, S. Sakashita, M. Sakashita, Y. Yasuda, S. Zaima, and S. Miyazaki, *Appl. Phys. Lett.* **85**, 5322 (2004).

⁴K. Kukli, M. Ritala, T. Pilvi, T. Sajavaara, M. Leskela, A. C. Jones, H. C. Aspinall, D. C. Gilmer, and P. J. Tobin, *Chem. Mater.* **16**, 5162 (2004).

⁵P. Rouffignac and R. G. Gordon, *Chem. Vap. Deposition* **12**, 152 (2006).

⁶L. Niinistö, M. Nieminen, J. Päiväsääri, J. Niinistö, M. Putkonen, and M. Nieminen, *Phys. Status Solidi A* **201**, 1443 (2004).

⁷M. Nieminen, M. Putkonen, and L. Niinistö, *Appl. Surf. Sci.* **174**, 155 (2001).

⁸S. Lütkehoff, M. Neumann, and A. Ślebarski, *Phys. Rev. B* **52**, 13808 (1995).

⁹A. Fissel, J. Dąbrowski, and H. J. Osten, *J. Appl. Phys.* **91**, 8986 (2002).

¹⁰D. D. Sarma and C. N. R. Rao, *J. Electron Spectrosc. Relat. Phenom.* **20**, 25 (1980).

¹¹J. S. Brinen, S. Greenhouse, and L. Pinatti, *Surf. Interface Anal.* **17**, 63 (1991).

¹²H. J. Osten, J. P. Liu, and H. J. Müssig, *Appl. Phys. Lett.* **80**, 297 (2002).